Rheol Acta (2007) 46:773–783
DOI 10.1007/s00397-007-0186-7

ORIGINAL CONTRIBUTION

# A study of viscoelasticity and extrudate distortions of wood polymer composites

**Velichko Hristov · John Vlachopoulos**

Received: 30 May 2006 / Accepted: 15 March 2007 / Published online: 3 April 2007


**Abstract** Natural fiber composites exhibit a characteristic surface tearing and extrudate distortions upon exiting from extrusion dies. This type of defect is characterized by highly rough, cracked, and distorted extrudate surface. In this study, the extrudate distortions and viscoelastic nature of metallocene-catalyzed polyethylene (mPE)/wood flour composites have been investigated. As the wood flour loading increases the region of linear viscoelasticity shortens. The first normal stress difference decreases, while the storage modulus increases. It was observed that increasing the wood flour loading up to 50 wt% aggravated the surface tearing; however, 60 wt% wood flour in mPE completely eliminated the surface defect. It was also found that increasing the shear rate improved the surface appearance of the filled compounds. This is due to the increased wall slip velocity of the composites at high shear rates and wood filler loadings. Increasing the diameter of the die at the same aspect ratio generally provides more severe surface tearing.

**Keywords** Wood polymer composites · Viscoelasticity · Sharkskin · Surface tearing

## Introduction

Wood-polymer composites (WPC) and in general natural fiber composites (NFC) have received considerable attention during the last decade. Their popularity stems from the fact that natural fillers represent low-cost renewable reinforcements that enhance mechanical properties such as stiffness, strength, and heat deflection temperature under load (Bledzki and Gassan 1999). NFC are widely used for decking and automotive applications, as well as a building material, where the relatively low density of the natural fillers is a major advantage. Most of the work being done on WPC/NFC is dedicated to investigation of the impact fracture and deformation behavior as well as influence of various additives on the mechanical properties, aging and durability (Raj et al. 1990). Along with the improvements that wood fillers bring to the matrix polymer, their addition also results in reduced ductility and poor impact resistance (Hristov et al. 2004). Furthermore, addition of wood fillers to thermoplastic polymers is accompanied by a considerable increase in the melt viscosity (Maiti and Hassan 1989; Maiti et al. 2004; Charlton et al. 2000; Li and Wolcott 2004–2006). The increased viscosity creates miscellaneous processing difficulties such as flow pulsations and extrudate surface defects upon exiting from the die.

In industrial WPC extrusions, the appearance of extrudates showing surface and edge tearing is well known since the inception of this technology in the 1980s. Although there are hundreds of publications on sharkskin and melt fracture phenomena involving neat polymers, there is little information on surface irregularities in extrusion of filled polymers. Goettler et al. (1982) observed significant surface and edge tearing of cellulose fiber-filled rubbers with increasing extrusion speed. According to the authors, this effect can be explained by the generation of weak shear planes within the short fiber composite, which forces the fibers lying near the die wall at a slight angle to the flow to easily tear upon emerging from the die. George et al. (1996) have also reported, for short pineapple fiber-reinforced low-

This paper was presented at the 3rd Annual Rheology Conference, AERC 2006, April 27–29, 2006, Crete, Greece.

V. Hristov · J. Vlachopoulos (✉)
Department of Chemical Engineering,
McMaster University,
1280 Main St. West,
Hamilton, ON L8S 4L7, Canada
e-mail: vlachopj@mcmaster.ca

density polyethylene (LDPE) composites, that the extrudates exhibit surface irregularities at high shear rates. Contrary to Goettler's and George's results, Becraft and Metzner (1992), Knuttson et al. (1981), Wu (1979), and Crowson et al. (1980) observed for different fiber-filled polymers much smoother extrudate surface at high shear rates rather than at low shear rates. The smoothness of the extrudates at high shear rates was attributed to fiber orientation in the direction of flow (Knuttson et al. 1981), normal stress effects, and rotation of fibers in the velocity field (Wu 1979). On the other hand, Birinci and Kalyon (2006) have observed that flow instabilities and extrudate distortions of poly (dimethyl siloxane), PDMS, filled with glass spheres could be eliminated upon the incorporation of particles at 40% by volume. The same authors have also shown that the die entry angle does not generate any differences in the flow behavior.

The importance of wall slip on flow instabilities and extrudate distortions of polymers has been discussed by many researchers (Ramamurthy 1986; Hatzikiriakos and Dealy 1992; Li and Wolcott 2004; Migler 2005). Using a continuous shear roll extruder, Kalyon et al. (2004) have observed that the high-density polyethylene (HDPE) melt detaches from both roll surfaces when the shear stress in the nip region between the two rolls surpasses the critical shear at which strong slip occurs. Similarly to the results of Kalyon et al. (2004), in a previous investigation on the extrudate surface tearing of wood flour-filled HDPE (Hristov et al. 2006), it was observed that wall slip helped to reduce the severity of the surface defects, and strong wall slip eliminated the extrudate surface tearing.

In the present investigation, a parallel plate rotational rheometer is used to characterize rheologically different formulations of a metallocene-catalyzed polyethylene (mPE) and wood flour (WFl). The compounds at various loadings of wood flour from 0 to 60 wt% are extruded through a capillary viscometer equipped with different dies and the extrudate appearance is examined.

## Experimental

### Materials and methods

mPE was employed as a matrix. This polyethylene has a melt index (MI) 4.0 g/10 min (190 °C/2.16 kg) and narrow molecular weight distribution (MWD; $M_w/M_n$ is less than 3). Maple wood flour, donated by Ontario Sawdust Supplies (Canada), having particle size within 100–150 μm, density of 1.5 g/cm$^3$, and relative moisture 6% was used as a filler. The wood particles have irregular to fiber-like shape with relatively low aspect ratio of 2–5. Figure 1 shows a scanning electron micrograph of the untreated wood flour. The wood particles surface is rough (see the insert in Fig. 1), and no filler aggregation occurred during compounding at any filler loading. To reduce the relative moisture below 0.5% wood flour was vacuum dried at 100 °C for 8 h before compounding. Wood-filled mPE composites containing 5, 10, 20, 30, 50, and 60 wt% (3.3÷40 vol%) wood flour were compounded on a HAAKE Rheomix 3000 internal mixer. The temperature of mixing was 170 °C, at rotor speed 50 rpm for 10 min mixing time. The composite formulations are given in Table 1.

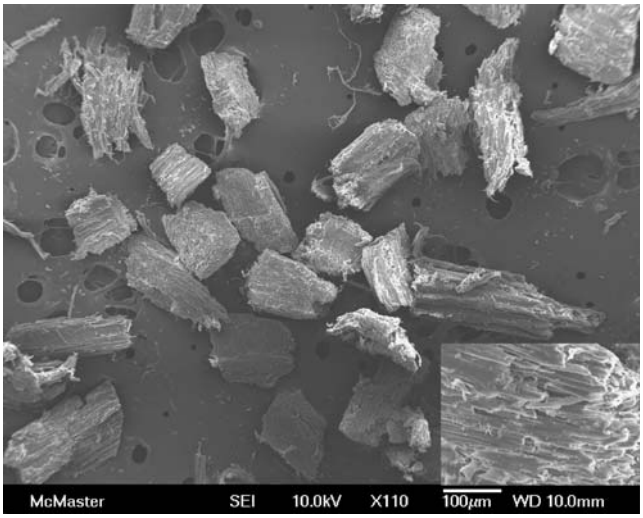


**Fig. 1** Scanning electron micrograph of wood flour. The *insert* shows the wood particle surface at higher magnification (×370)

### Capillary viscometry

Capillary rheometer Rosand Precision 700 equipped with different sets of dies was employed to collect experimental data for the pressure drop and volume flow rate. Since it was known from a previous investigation (Hristov et al. 2006) that PE/wood flour composites exhibit slip at the wall, no attempt was made to apply the well-known Rabinowitsch and Bagley corrections (Dealy and Wissburn 1990). All results are reported in terms of apparent shear rate and nominal wall shear stress given by the following equations, respectively:

$$\dot{\gamma}_a = \frac{4Q}{\pi R^3}, \tag{1}$$

$$\tau_w = \frac{\Delta P}{2L} R, \tag{2}$$

where $Q$ is the volumetric flow rate, $\Delta P$ is the pressure drop in capillary, and $L$ and $R$ are the length and radius of the die, respectively. All measurements were performed at 180 °C temperature.

**Table 1** Composites formulation

| Composite code | mPE, wt% | WFl, wt% |
|---|---|---|
| mPE | 100 | – |
| mPE5 | 95 | 5 |
| mPE10 | 90 | 10 |
| mPE20 | 80 | 20 |
| mPE30 | 70 | 30 |
| mPE50 | 50 | 50 |
| mPE60 | 40 | 60 |

Dies having same diameter of 1.0 mm but different aspect ratio $L/D$ of 8, 16, 24, and 32, and three dies with the same aspect ratio of $L/D$=16 and diameter 1.0, 1.5, and 2.0 mm were used in this research. Dimensions of the dies are given in Table 2. Extrudates at different shear rates were collected and after solidification were examined under an *Olympus CZ-60* light microscope equipped with *Panasonic BP-310* digital camera for the purpose of photographing the extrudate surface defects.

## Rotational rheometry

Measurements in both steady and dynamic oscillatory mode were performed on a parallel plate TA Instruments ARES rheometer under strain-controlled conditions. The plates diameter is 25 mm and the gap between plates was set to 1.5 mm. 2-mm thick disc test samples having the same diameter as the rheometer plates were prepared by compression molding at 180 °C for 10 min overall compression time. The samples were put between the plates and heated to 180 °C for 3 min to eliminate previous thermal history. After adjusting the gap to 1.5 mm, the squeezed molten material was carefully trimmed off for attaining smooth edge surface. Dynamic frequency sweeps were carried out from 0.1 to 100 rad/s range at a strain within the linear viscoelastic region (LVR) of the materials. Measurements bellow 0.1 rad/s were not performed because the time for reaching steady state at very low frequencies considerably increased (about an hour at 0.01 rad/s). Extensive thermal degradation of the highly filled materials, which can be even visually observed, would make the frequency sweeps questionable. The strain amplitude being applied during the frequency sweeps was determined in a separate dynamic strain sweep test within 0.01–100% at a constant frequency of 10 rad/s. Each measurement was performed on a fresh compression-molded sample, and repeated measurements had been conducted to ensure the reproducibility of the experimental results.

**Table 2** Dimensions of the dies

| Die number | Length, mm | Diameter, mm | $L/D$ |
|---|---|---|---|
| 1 | 8 | 1 | 8 |
| 2 | 16 | 1 | 16 |
| 3 | 24 | 1 | 24 |
| 4 | 32 | 1 | 32 |
| 6 | 16 | 1 | 16 |
| 7 | 24 | 1.5 | 16 |
| 8 | 32 | 2 | 16 |

The parallel plate rheometer oscillates one plate at amplitude of $\phi_0$ and measures the torque $M_0$, and phase lag $\delta$. The storage modulus, $G'$, and loss modulus, $G''$, are calculated according to the following equations (Dealy and Wissburn 1990):

$$G' = \frac{2M_0 h}{\pi R^4 \phi_0} \cos\delta, \tag{3}$$

$$G'' = \frac{2M_0 h}{\pi R^4 \phi_0} \sin\delta, \tag{4}$$

and the complex viscosity, $\eta^*$, is calculated as:

$$\eta^* = \sqrt{\left(\frac{G'}{\omega}\right)^2 + \left(\frac{G''}{\omega}\right)^2}, \tag{5}$$

where $R$ is the plate radius, $h$ is the gap between plates, and $\omega$ is the frequency.

Steady shear measurements were performed within 0.01–10 $s^{-1}$ shear rate interval and the shear rate $\dot{\gamma}_a$ (at $r = R$), shear stress $\tau_w$, and the first normal stress difference $N_1 = (\tau_{11} - \tau_{22})$ were calculated according to the following equations, respectively (Macosko 1994):

$$\dot{\gamma}_a = \frac{R\Omega}{h}, \tag{6}$$

$$\tau_w = \frac{2M_0}{\pi R^3}, \tag{7}$$

$$N_1 - N_2 = \frac{F_z}{\pi R^2}\left[2 + \frac{dInF_z}{dIn\dot{\gamma}_a}\right], \tag{8}$$

where $F_z$ is the total thrust, $N_1 = (\tau_{11} - \tau_{22})$ and $N_2 = (\tau_{22} - \tau_{33})$ are the first and second normal stress differences respectively, and $\Omega$ is the angular velocity.

## Wall slip analysis

Wall slip measurements were carried out on the same capillary rheometer following the Mooney technique (Mooney 1931). Normally, the rheometer calculates the shear rate from the volume flow rate and die dimensions by

assuming that the fluid velocity at the die wall is zero. With an appropriate choice of dies, several sets of data can be combined to provide a slip correction. The aspect ratio of the dies is kept constant to ensure that the pressure drop is nearly uniform in all experiments and to avoid variations on the slip velocities due to pressure effects (Hatzikiriakos and Dealy 1992).

Three dies having 1.0, 1.5, and 2.0 mm diameter and $L/D$= 16 are used, and the wall shear stress data are collected at shear rates 20–500 $s^{-1}$. Measurements at shear rates lower than 20 $s^{-1}$ were not performed because of the significantly increased time for achieving steady state, which would probably cause material degradation and structure alterations giving erroneous results. Measurements at shear rates above 500 $s^{-1}$ were not performed due to flow instabilities and pressure fluctuations already discussed elsewhere (Hristov et al. 2006).

For a system with slip, the total volume flow rate, $Q$, through the die is given by the following equation (Dealy and Wissburn 1990; Archer 2005):

$$Q = \frac{\dot{\gamma}_T \pi R^3}{4} + \pi R^2 V_s, \tag{9}$$

where $R$ is the die radius, $\dot{\gamma}_T$ is the true slip-corrected shear rate, and $V_s$ is the slip velocity. The apparent shear rate, $\dot{\gamma}_a$, given by Eq. 1, and combined with Eq. 9 gives

$$\dot{\gamma}_a = \dot{\gamma}_T + \frac{4V_s}{R}, \tag{10}$$

It is clear that if plotting $\dot{\gamma}_a$, against $1/R$, for certain shear stress, the intercept on the $y$-axis gives the slip-corrected shear rate $\dot{\gamma}_T$ and the slope is $4V_s$.

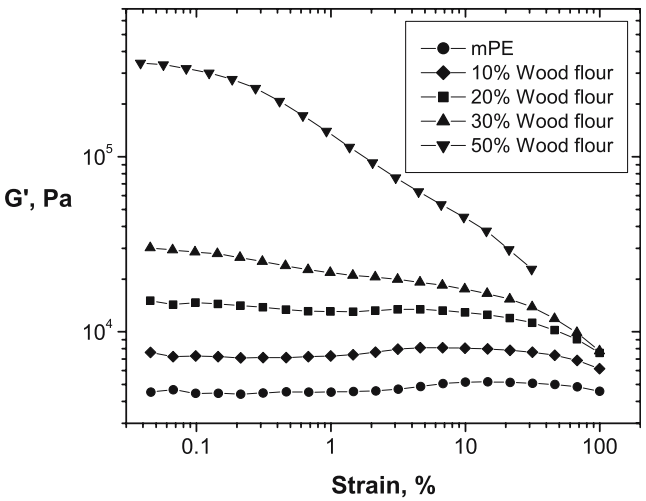


**Fig. 2** Storage modulus dependence on the dynamic strain of wood filled mPE (frequency 10 rad/s)

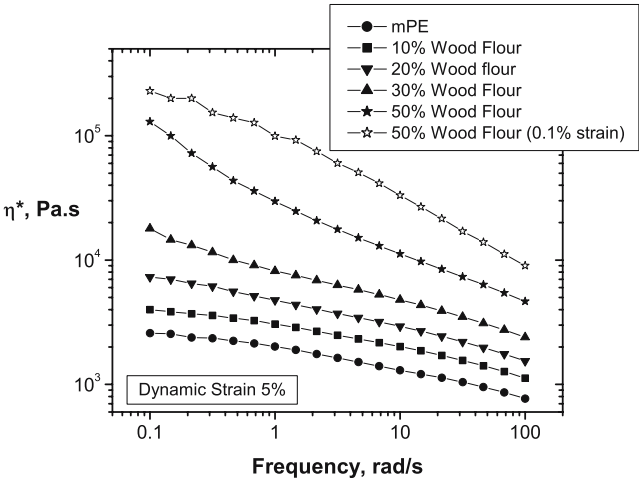


**Fig. 3** Complex viscosity versus frequency of wood filled mPE

## Results and discussion

Strain-sweep experiments were performed first, and the results are shown in Fig. 2. It can be seen in Fig. 2 that the storage modulus, $G'$, of the neat mPE does not change within the entire strain range. Moderate filled composites (up to 20% wood flour) showed relatively high resistance to deformation as well. At strains above 60%, however, it is seen that $G'$ decreases, which is a sign of possible change in the composite structure. It is interesting to note here that the strain, at which the storage modulus sharply drops down, decreases from about 70% for the 20 wt% wood filled composite to nearly 0.1% for the 50 wt% filled mPE. These results are fully in agreement with the results of Marcovich et al. (2004) and Li and Wolcott (2006) for wood filled polymer composites. The reduction in the storage modulus with increase of the strain is an indication of breakage of the material structure. This behavior is similar to that of

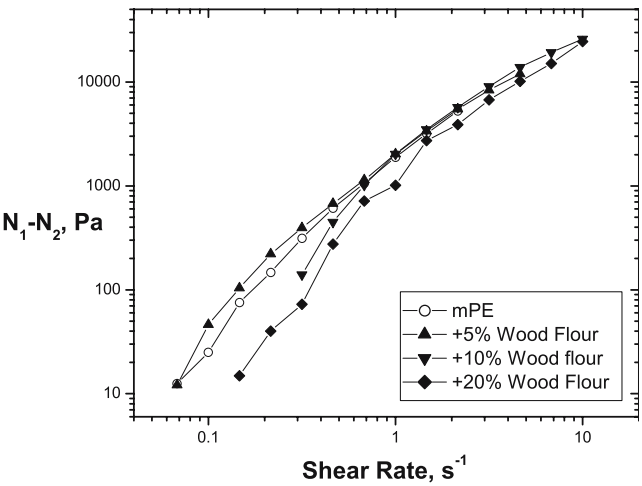


**Fig. 4** Variation of $N_1$–$N_2$ with apparent shear rate for wood filled mPE

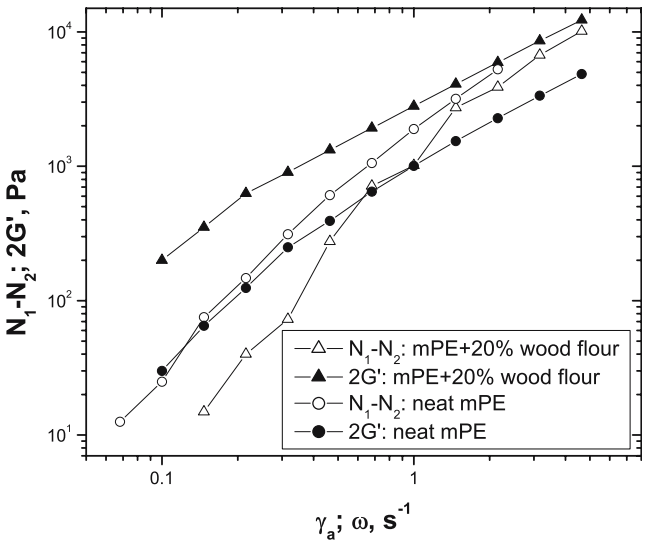


**Fig. 5** $2G'$ versus frequency and $N_1$–$N_2$ versus shear rate for 0 and 20% wood filled mPE

filled rubbers in dynamic mechanical analysis and known as the Payne effect (Payne 1960). The reason for the structure breakage at high dynamic strains could be attributed to the incompatibility and poor adhesion between the matrix and natural fillers (Saheb and Jog 1999). Progressively increasing strain generates high shear stresses that cannot be transferred through the interface (because of the poor adhesion), and the deformation energy cannot be effectively absorbed by the filler particles.

The complex viscosity dependence on the frequency is illustrated in Fig. 3. In this set of experiments, 5% dynamic strain was selected. It is seen from Fig. 2 that this strain lies within the LVR of 0–30 wt% filled composites. For the 50 wt% wood filled composite mPE50, however, 5% strain is outside the LVR. It is clearly seen in Fig. 3 that neat mPE and moderately filled composites exhibit typical for polymers viscosity dependence on the frequency, namely, Newtonian plateau at low frequencies and shear thinning at high frequencies. The complex viscosity–frequency curve at 5% strain for the 50 wt% composite has no Newtonian plateau and lies far below the respective viscosity data taken at a strain within its LVR (0.1% strain). It is apparent that at 5% dynamic strain, the composite structure is getting broken during the test, and thus, the system experiences less resistance to shearing.

It is clearly observed in Fig. 3 that moderate increase of the wood flour loading (up to 20 wt%) provides almost the same degree of shear thinning as in the neat mPE (the curves are parallel to each other), but at higher loadings, the Newtonian plateau tends to disappear, except that the measurements at 0.1% dynamic strain indicate a small tendency for Newtonian plateau.

It has been reported that the first normal stress difference ($N_1$) significantly increases with increasing the fiber loading

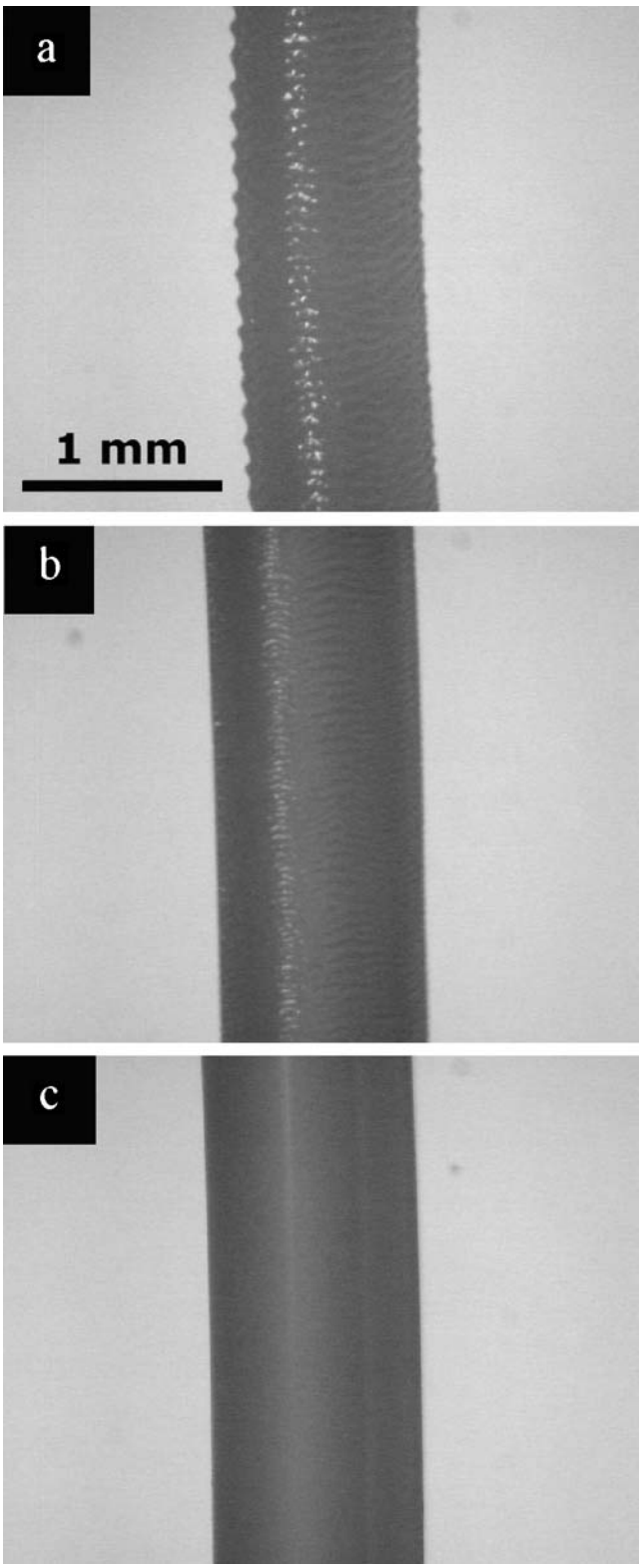


**Fig. 6** Extrudates surface morphology of neat mPE in dependence of $L/D$ of the die: **a** $L/D$=8, **b** $L/D$=24, **c** $L/D$=32; $D$=1.0 mm; $\dot{\gamma}_a = 250\,s^{-1}$

(Chan et al. 1978; White et al. 1980). The large increase in the normal stresses of fiber-filled polymers was attributed to a hydrodynamic particle effect, associated with orientation in the direction of flow (White et al. 1980). On the contrary, it has been shown (Han 1976) that the presence of particulate fillers decreases the elasticity of the polymer. Moreover, it has also been demonstrated (Charlton 2001) that the extrudate swell of rice hulls-filled HDPE decreases with increasing the filler content, which was attributed to decreased elasticity. For neat polymer melts, it is known that the second normal stress difference $N_2 \approx -0.2N_1$ (Macosko 1994), but Ohl and Gleissle (1992) have reported that for highly concentrated suspensions (limestone in polyisobutene), the second normal stress difference is higher than the first normal stress difference. Large negative values of the first normal stress difference have been observed by Aral and Kalyon (1997) for PDMS/hollow glass spheres suspensions, and Laun (1994) found negative normal stress difference values for colloidal spheres in a Newtonian binder.

The dependence of $N_1$–$N_2$ on the shear rate is shown in Fig. 4. It can be seen in Fig. 4 that at the same shear rate $N_1$–$N_2$ decreases (except for the 5 wt% loading) with increasing the wood flour loading.

In the linear viscoelasticity region $2G'$ should be equal to $N_1$ at very low shear rate/frequency (Macosko 1994). It is seen in Fig. 5 that for the neat mPE, the $N_1$–$N_2$ difference and $2G'$ data nearly coincide at low shear rates/frequencies (0.1–0.3 $s^{-1}$) and at shear rates above 0.3 $s^{-1}$ $N_1$ becomes larger than $2G'$. Similar results for the 5 wt% filled mPE were also obtained (but not shown in the graph) indicating that wood flour in low weight percentage does not alter significantly the viscoelastic properties of the neat resin. For the 20 wt% filled mPE at low shear rates, however, $N_1$–$N_2$ is much lower than $2G'$ at low shear rates/frequencies (0.1–0.4 $s^{-1}$), which means that at lower shear rates, $N_2$ probably is of the same magnitude as $N_1$. Increasing the wood flour loading above 20 wt% generated negative normal force readings at all shear rates (not shown in Fig. 5). It could be speculated that at high filler loadings, the second normal stress difference $N_2$ is really becoming higher than $N_1$ supporting the results of Ohl and Gleissle (1992), or that $N_1$ is negative as Aral and Kalyon (1997) and Laun (1994) have found. With our parallel plate rheometer, it is not possible to differentiate. However, since we measured positive values of the extrudate swell (less than with the neat polymer) in other independent experiments for the same filler loadings, we believe that $N_1$ remains positive.

The second part of this study concerns the extrudate distortion dependence on the wood flour loading and die

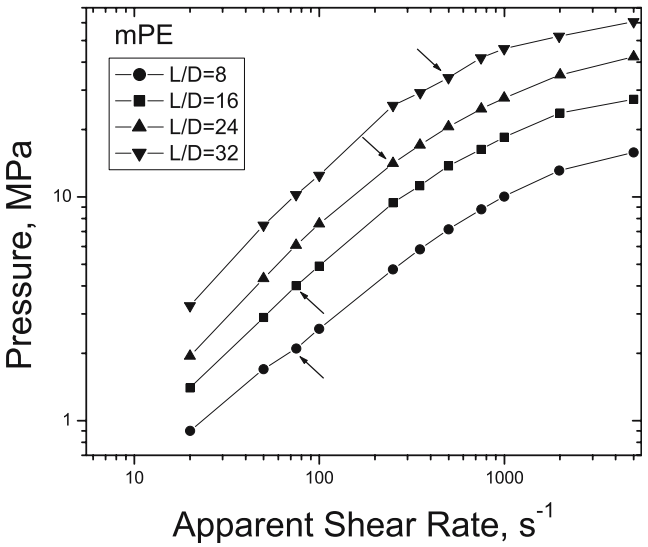


**Fig. 7** Flow curves of the neat mPE as a function of $L/D$ of the die (*arrows* indicate the onset of sharkskin)

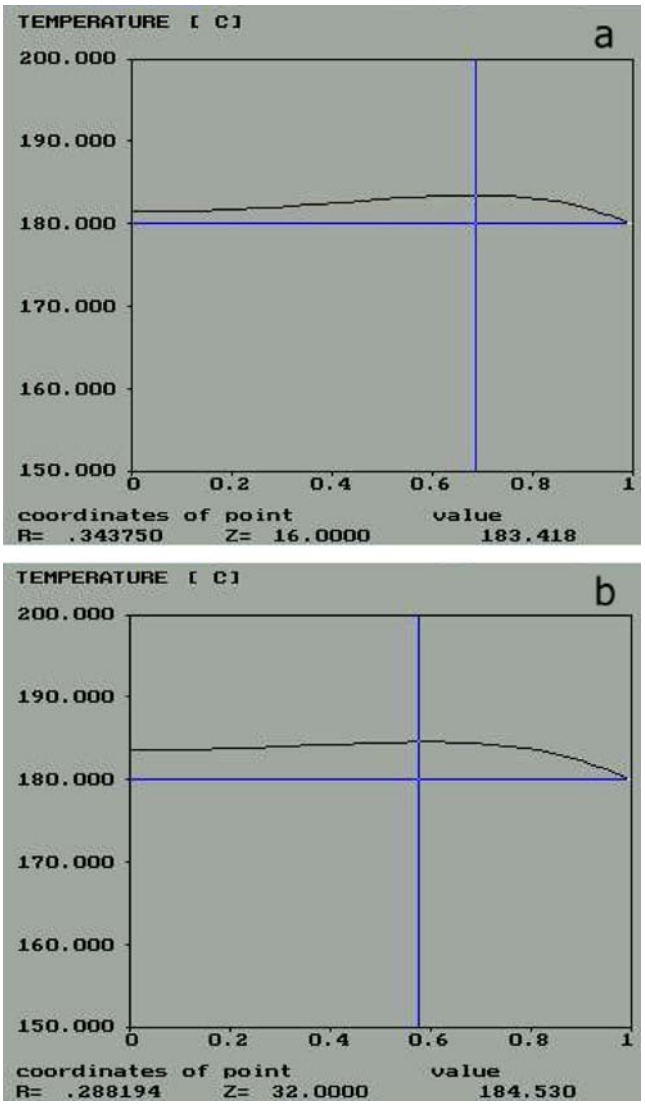


**Fig. 8** Temperature profile of the neat mPE entering at 180 °C at position along the die length: **a** $z$=16 mm, **b** $z$=32 mm. Die wall kept at 180 °C; $L/D$=32, $D$=1.0 mm, $\dot{\gamma}_a = 500\,s^{-1}$

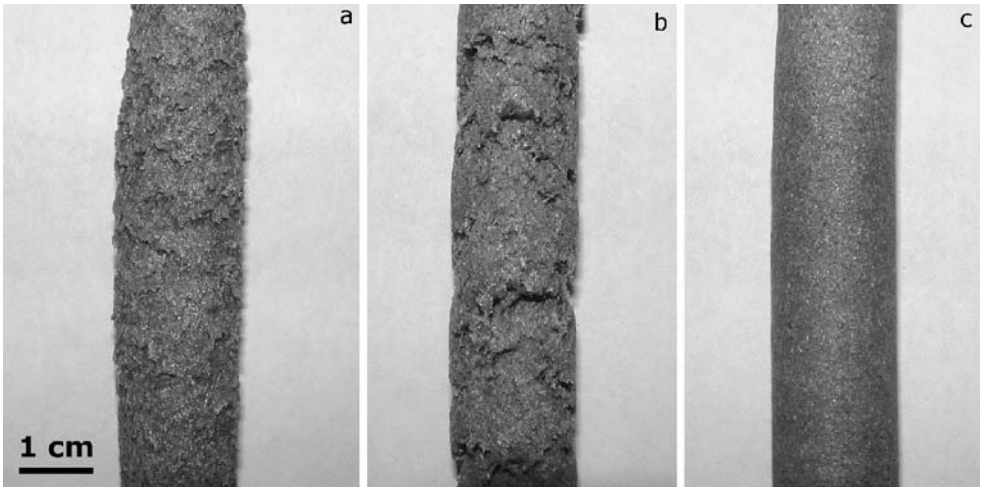


**Fig. 9** Extrudate surface morphology of wood filled mPE-open barrel experiments, $L/D$=6; $D_b$=15 mm, $\dot{\gamma}_a = 2.5\,s^{-1}$: **a** 30% filler, **b** 50% filler, **c** 60% filler

geometry. The extrudate surface morphology of the neat mPE in dependence on the aspect ratio of the die is illustrated in Fig. 6. Metallocene PE exhibits the usual for the linear polyolefins flow behavior, namely, smooth extrudate surface at low shear rates, sharkskin at moderate shear rates, and melt fracture at high shear rates (Vlachopoulos and Alam 1972; Denn 2001). It can be seen in Fig. 6 that, at the same shear rate of 250 $s^{-1}$, the severity of sharkskin diminishes with increasing $L/D$ of the die (nonexistent with $L/D$=32 die, Fig. 6).

Figure 7 illustrates the pressure drop in capillaries with different $L/D$ ratio as a function of the apparent shear rate, and arrows on the plot indicate the onset of sharkskin of neat mPE as observed in the light microscope. It is seen that the aspect ratio of the die has a significant influence on the flow behavior of mPE. The onset of sharkskin moves toward higher apparent shear rates when extruding through longer dies. These results are in agreement with the results of Moynihan et al. (1990), who reported a decrease in sharkskin severity with an increase of $L/D$ from 12.5 to 75. Ballenger et al. (1971) also observed that sharkskin effect was more pronounced in shorter capillaries of small diameter. Opposite to Ballenger and Moynihan, Kurtz (1984), Beaufils et al. (1989), and Fujiyama and Inata (2002) found no effect of $L/D$ on the sharkskin effect. Venet and Vergnes (1997) have also reported for metallocene narrow MWD polyethylene that the amplitude of the sharkskin is quite independent of the die length. Migler (2005) reconciled

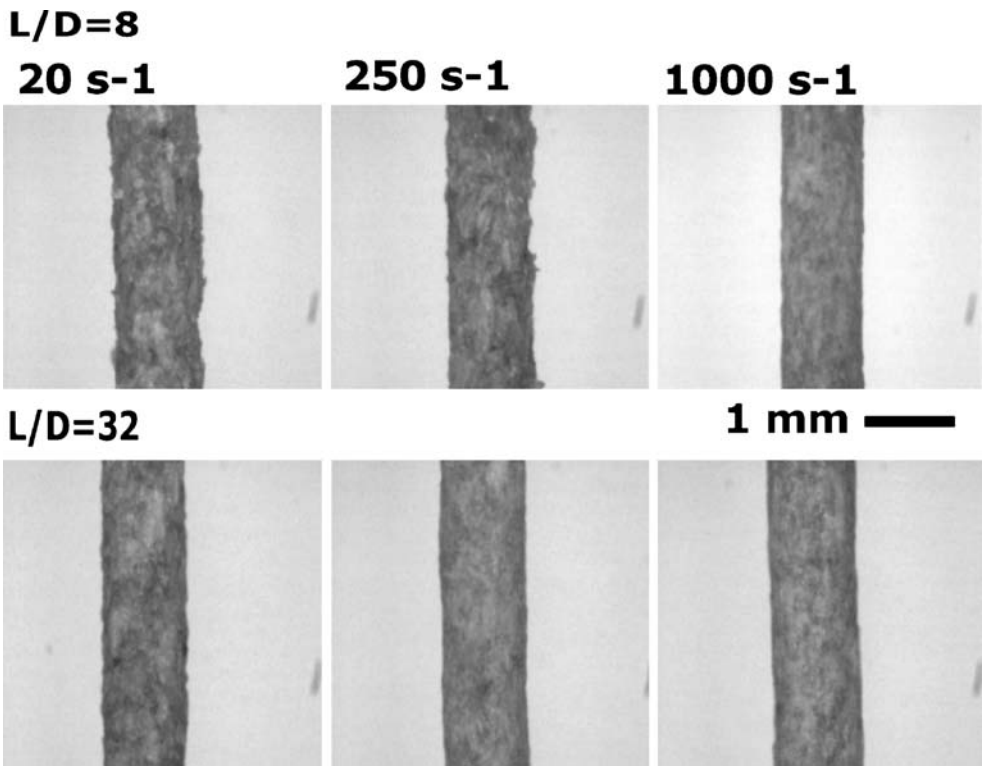


**Fig. 10** Extrudate surface morphology of 60-wt% wood filled mPE composites in dependence on $L/D$ of the die at different apparent shear rates; $D$=1 mm

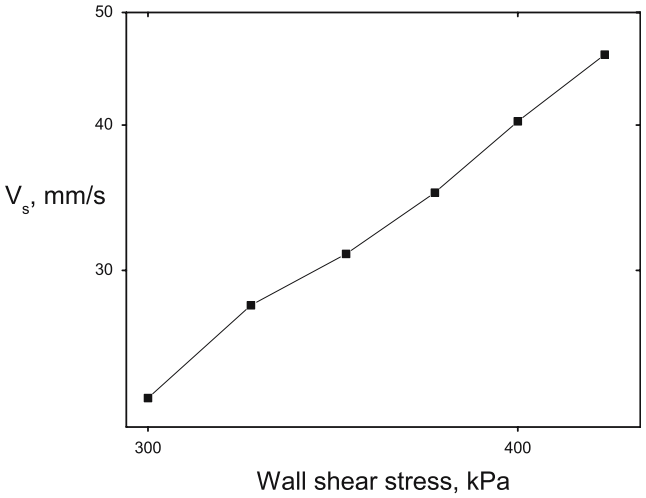


**Fig. 11** Wall slip velocity dependence on the wall shear stress of 50% filled mPE

these two different results by noting "in the experiments where no effect of length was found, *L*/*D* ranges from 4 to 20, whereas in the case of Moynihan, the *L*/*D* values vary from 12 to 75. Thus, perhaps the difference between two cases is that there is fully developed flow in the latter."

The present authors believe that the dependence of sharkskin on length of the capillary is probably due to viscous dissipation effects. For short capillaries, there is hardly any temperature rise due to viscous heating. For long capillaries, the adiabatic temperature rise (converting the mechanical energy into heat) can be calculated by

$$\Delta PQ = \rho Q C_p \Delta T \; or \; (\Delta T) = \frac{\Delta P}{\rho C_p}, \tag{11}$$

At pressure levels of about 45 MPa, for material with melt density $\rho$=780 kg/m$^3$ and heat capacity $C_p$=2,300 J/kg°C, we get an adiabatic temperature rise of about 25 °C. For steady flow at shear rate of 500 s$^{-1}$ and with constant wall temperature 180 °C, the temperature rise at the die exit was also calculated for neat mPE using FEM software to be 4.5 °C (temperature profiles shown in Fig. 8). However, in the short period of the piston extrusion experiment, the conditions are likely to be closer to adiabatic than constant wall temperature. Lawal and Kalyon (1997) have reported that isothermal condition underpredicts the temperature rise and the adiabatic condition overpredicts it. In the present case, we would expect a temperature rise between 4.5 and 25 °C. This large temperature rise is responsible for viscosity decrease and postponement of sharkskin to higher shear rates (Miller and Rothstein 2004).

It is well known within the rubber industry that increasing the carbon black loading and specific area of carbon black particles helps to avoid extrudate distortions (Cotten 1979). It should be mentioned here that the beneficial effect of the reinforcing fillers has been exploited

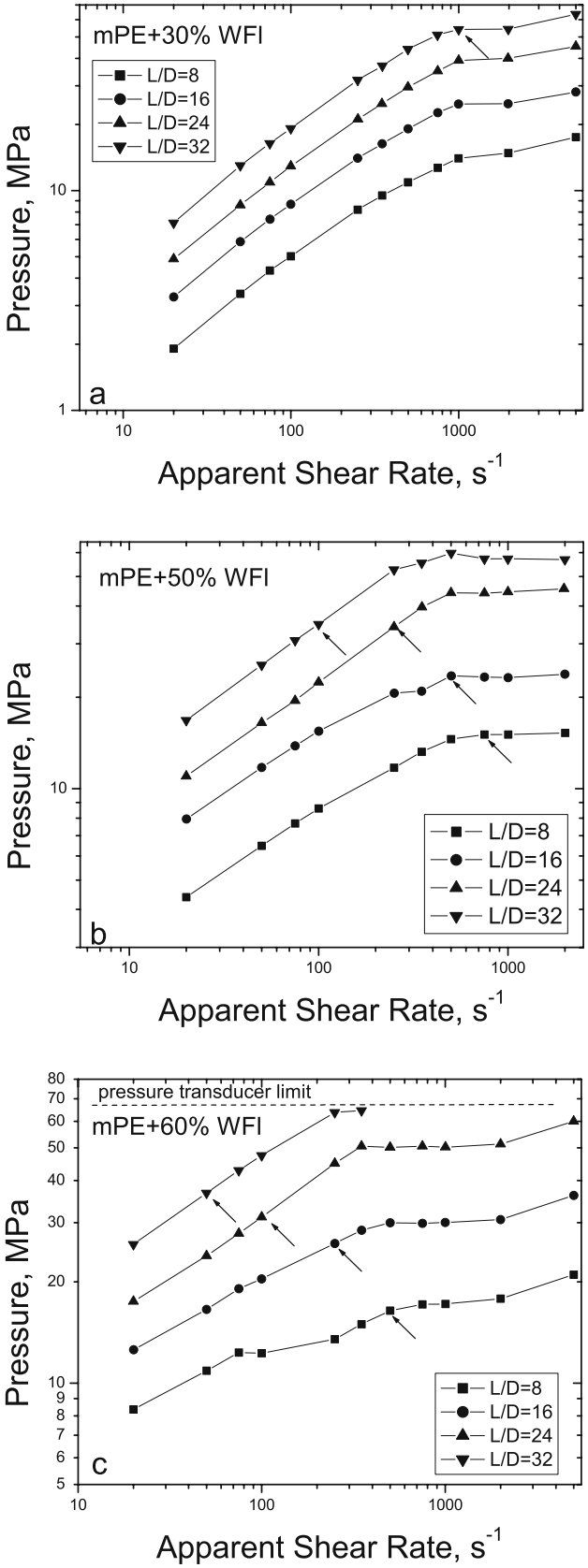


**Fig. 12** Flow curves of wood filled mPE composites: **a** 30%, **b** 50%, **c** 60%. *Arrows* indicate the onset of smooth extrudate extrusion

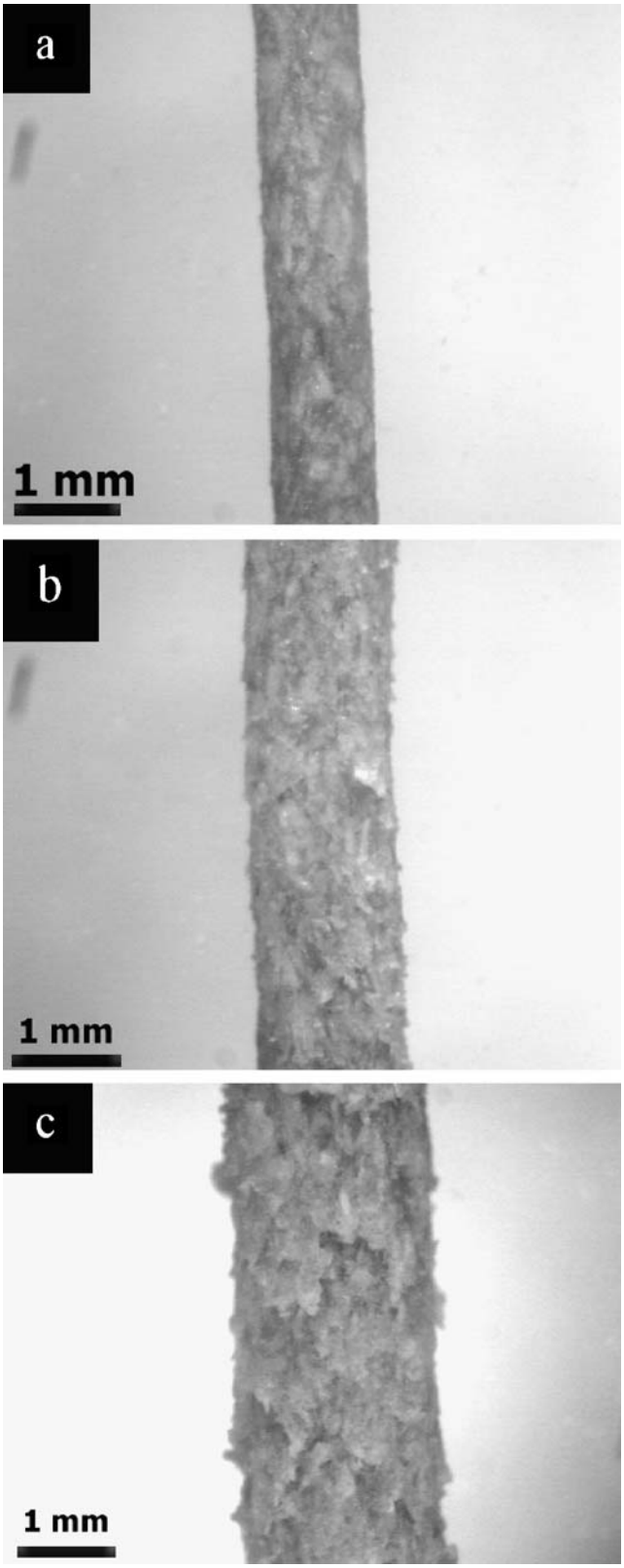


**Fig. 13** Extrudate surface morphology of 50% wood filled mPE composite in dependence on die diameter: **a** $D$=1.0 mm, **b** $D$=1.5 mm, **c** $D$=2.0 mm; $\dot{\gamma}_a = 20\,s^{-1}$, $L/D$=16

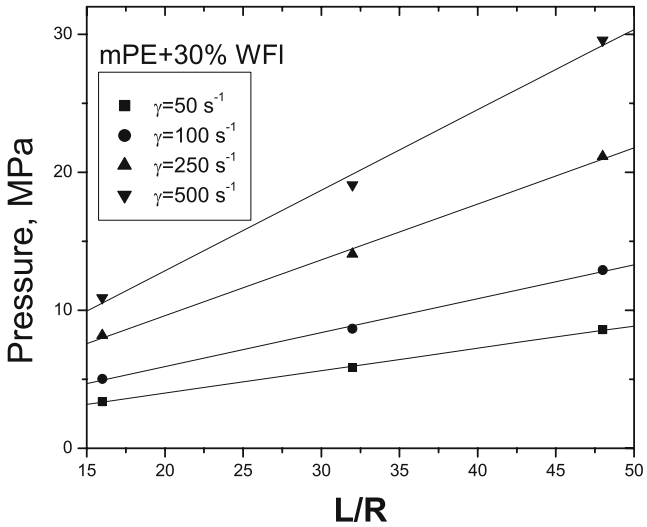


**Fig. 14** Bagley plots of 30 wt% filled mPE

in the polymer industry for long; however, it has received very little research interest (Leblanc 2002; Birinci and Kalyon 2006). The effect of the filler concentration on the evolution of the extrudate surface tearing is illustrated in Fig. 9. These extrudates were obtained by extrusion of the composites through the rheometer barrel with no die attached. In that way, the effect of the die entrance on the surface tearing effect would be excluded. It can be seen from the figure that at apparent shear rate of 2.5 $s^{-1}$, the surface tearing effect aggravates with increasing the filler content from 30 to 50 wt% (Fig. 9a and b), and further at 60 wt% wood flour loading, the defect disappears (Fig. 9c). The neat mPE and composites with wood flour concentration up to 20 wt% do not show any significant surface defects or tearing upon extrusion at shear rate of 2.5 $s^{-1}$ and are not shown in Fig. 9.

Figure 10 illustrates the morphological features of the 60 wt% wood filled mPE in dependence on the $L/D$ of the die at different apparent shear rates. Figure 10 reveals that increasing the aspect ratio of the die results in smoother extrudates. The other composites exhibit similar behavior. In addition, it is seen from Fig. 10 that a higher shear rate is beneficial for the production of smoother extrudates. This is probably due to the wall slip effect in capillary flow. Figure 11 illustrates the dependence of the wall slip velocity on the wall shear stress of the 50 wt% filled composite calculated according to Eq. 10. It is seen in Fig. 11 that the wall slip velocity increases with shear stress, which is likely the reason for obtaining smoother extrudates with increasing shear rate. The other composites also exhibit the same trend and the results are in agreement with the results from our previous investigation on the phenomenon of slip at the wall in wood filled polyethylene (Hristov et al. 2006).

Figure 12 shows the pressure in capillaries versus shear rate of wood filled mPE composites as a function of $L/D$ of

the dies. It can be seen from Fig. 12 that the pressure is increasing with shear rate, and after a certain apparent shear rate, the pressure remains constant. This is obvious for all wood filled composites extruded through all dies. The arrows in the graphs indicate the pressure (shear rate respectively) of obtaining smooth extrudates. It can be seen that the shear rate for smooth extrudate surface decreases with both increasing the $L/D$, and wood flour loading, namely, longer dies and high filler content widen the shear rate range for smooth extrudate extrusion. The observation that the extrudates are becoming smoother with increasing the filler loading is fully in agreement with the experiments of Birinci and Kalyon (2006) for PDMS filled with 40 vol% hollow glass spheres.

In addition to the effect of die length, it was found that extrudate surface tearing depends on the die diameter. The extrudate surface morphology dependence on the die diameter is shown in Fig. 13. It can be seen that during extrusion of 50 wt% filled mPE (the other composites showed similar trend), the extrudates emerge from the 1-mm diameter die with much smoother surface whereas increasing the die diameter results in tearing of the extrudates. The most severe extrudate tearing and surface roughness were observed in the case of flow through the 2-mm diameter die.

Bagley plots, namely pressure drop in capillary ($\Delta P_c$) versus length to die radius ratio ($L/R$) were obtained from the raw data, and the results for the 30 wt% filled mPE are shown in Fig. 14. The pressure data were collected within 20–500 $s^{-1}$ shear rates due to flow instabilities and pressure fluctuations at higher shear rates (the plateau region in Fig. 12). The entrance pressure drop increases with increasing the shear rate, and the linearity of the plots for mPE and filled composites containing up to 30 wt% filler holds in capillaries with L/R ratio up to 48. Increasing the wood flour content leads to significant deviation from linearity, particularly at high shear rates and long capillaries, making the Bagley procedure for evaluation of the entrance pressure loss invalid.

The present results support the hypothesis that increased wall slippage is responsible for obtaining smoother extrudates at high filler content. However, there might be other mechanisms involved such as compressibility at very high pressures and viscous dissipation at high flow rates.

## Conclusions

The viscoelastic nature of polyethylene/wood flour composites was investigated by rotational rheometry. It was found that as the loading of wood flour increases, the region of linear viscoelasticity shortens. The first normal stress difference significantly decreases with filler loading while the storage modulus increases.

It was observed that WPC exhibit characteristic surface tearing upon exiting from the die even at very low shear rates. The surface tearing is eliminated at higher shear rates and very high loading (60 wt%) of wood flour. Increasing the aspect ratio of the die diminishes the severity of the extrudate surface tearing, but increasing the die diameter at the same $L/D$ worsens the surface defect.

**Acknowledgement** The authors would like to thank Dr. D. Strutt for performing the FEM numerical calculations. Financial supports from McMaster Manufacturing Research Institute (MMRI) and the Extrusion Division of the Society of Plastics Engineers (Lew Erwin Memorial Scholarship to V. Hristov) are also gratefully acknowledged.

## References

Aral BK, Kalyon DM (1997) Viscoelastic material functions of noncolloidal suspensions with spherical particles. J Rheol 41:599–620

Archer LA (2005) Wall slip: measurements and modeling issues in "polymer processing instabilities-control and understanding." Hatzikiriakos SG, Migler KB (eds) Dekker, New York

Ballenger TF, Chen IJ, Crowder JW, Hagler GE, Bogue DC, White JL (1971) Polymer melt flow instabilities in extrusion: investigation of the mechanism and material and geometric variables. J Rheol 15:195–215

Beaufils P, Vergnes V, Agassant JF (1989) Characterization of the sharkskin defect and its development with the flow conditions. Int Polym Process 4:78–84

Becraft ML, Metzner AB (1992) The rheology, fiber orientation, and processing behavior of fiber-filled fluids. J Rheol 36:143–174

Birinci E, Kalyon DM (2006) Development of extrudate distortions in poly(dimethyl siloxane) and its suspensions with rigid particles. J Rheol 50:313–326

Bledzki AK, Gassan J (1999) Composites reinforced with cellulose based fibers. Prog Polym Sci 24:221–274

Chan Y, White JL, Oyanagi Y (1978) A fundamental study of the rheological properties of glass-fiber-reinforced polyethylene and polystyrene melts. J Rheol 22:507–524

Charlton Z (2001) Profile extrusion of highly filled cellulose–polyethylene composites, M.Eng. thesis, Department of Chemical Engineering, McMaster University, Hamilton, Canada

Charlton Z, Vlachopoulos J, Suwanda D (2000) Profile extrusion of highly filled recycled HDPE. Society of Plastics Engineers, Annual Technical Conference (ANTEC) 2914–2918

Cotten GR (1979) Significance of extensional flow in processing rubbers. Plast Rubber Proc 4:89–95

Crowson RJ, Folkes MJ, Bright PF (1980) Rheology of short glass fiber-reinforced thermoplastics and its application to injection molding I. Fiber motion and viscosity measurement. Polym Eng Sci 20:925–933

Dealy J, Wissburn KF (1990) Melt rheology and its role in plastics processing. Van Nostrand Reinhold, New York

Denn MM (2001) Extrusion instabilities and wall slip. Annu Rev Fluid Mech 33:265–287

Fujiyama M, Inata H (2002) Melt fracture behavior of polypropylene-type resins with narrow molecular weight distribution. I. Temperature dependence. J Appl Polym Sci 84:2111–2119

George J, Janardhan R, Anand J, Bhagawan S, Thomas S (1996) Melt rheological behaviour of short pineapple fibre reinforced low density polyethylene composites. Polymer 37:5421–5431

Goettler L, Sezna J, DiMauro PJ (1982) Short fiber reinforcement of extruded rubber profiles. Rubber World 187:33–42

Han CD (1976) Rheology in polymer processing. Academic, New York, p 182

Hatzikiriakos SG, Dealy JM (1992) Wall slip of molten high density polyethylenes. II. Capillary rheometer studies. J Rheol 36: 703–741

Hristov VN, Vasileva S, Krumova M, Lach R, Michler GH (2004) Deformation mechanisms and mechanical properties of modified polypropylene/wood fiber composites. Polym Compos 25:521–526

Hristov V, Takacs E, Vlachopoulos J (2006) Surface tearing and wall slip phenomena in extrusion of highly filled HDPE/wood flour composites. Polym Eng Sci 46:1204–1214

Kalyon DM, Gevgilili H, Shah A (2004) Detachment of the polymer melt from the roll surface: calendering analysis and data from a shear roll extruder. Int Polym Process 19:129–138

Knutson BA, White JL, Abbas K (1981) Rheological and extrusion characteristics of glass fiber-reinforced polycarbonate. J Appl Polym Sci 26:2347–2362

Kurtz SJ (1984) Die geometry solutions to sharkskin melt fracture. In: B Mena (ed) Advances in rheology. UNAM, Mexico, pp 399–407

Laun HM (1994) Normal stresses in extremely shear thickening polymer dispersions. J Non-Newton Fluid Mech 54:87–108

Lawal A, Kalyon DM (1997) Viscous heating in nonisothermal die flows of viscoplastic fluids with wall slip. Chem Eng Sci 52:1323–1337

Leblanc JL (2002) Rubber-filler interactions and rheological properties in filled compounds. Prog Polym Sci 27:627–687

Li TQ, Wolcott MP (2004) Rheology of HDPE-wood composites: I. Steady state shear and extensional flow. Composites Part A 35:303–311

Li TQ, Wolcott MP (2005) Rheology of wood plastics melt, part 1: capillary rheometry of HDPE filled with maple. Polym Eng Sci 45:549–559

Li TQ, Wolcott MP (2006) Rheology of wood plastics melt, part 3: non-linear nature of the flow. Polym Eng Sci 46:114–121

Macosko CW (1994) Rheology-principles, measurements, and applications. VCH, New York

Maiti SN, Hassan MR (1989) Melt rheological properties of polypropylene-wood flour composites. J Appl Polym Sci 37:2019–2032

Maiti SN, Subbarao R, Ibrahim MN (2004) Effect of wood fibers on the rheological properties of i-PP/Wood fiber composites. J Appl Polym Sci 91:644–650

Marcovich N, Reboredo M, Kenny J, Aranguren M (2004) Rheology of particle suspensions in viscoelastic media. Wood flour-polypropylene melt. Rheol Acta 43:293–303

Migler KB (2005) Sharkskin instability in extrusion. In: KB Migler, Hatzikiriakos S (eds) Polymer processing instabilities: control and understanding. Dekker, New York, pp 135–136

Miller E, Rothstein JP (2004) Control of the sharkskin instability in the extrusion of polymer melts using induced temperature gradients. Rheol Acta 44:160–173

Mooney M (1931) Explicit formulas for slip and fluidity. J Rheol 2:210–222

Moynihan R, Baird D, Ramanathan R (1990) Additional observations on the surface melt fracture behavior of linear low-density polyethylene. J Non-Newton Fluid Mech 36:255–263

Ohl N, Gleissle W (1992) The second normal stress difference for pure and highly filled viscoelastic fluids. Rheol Acta 31:294–305

Payne AR (1960) A note on the existence of a yield point in the dynamic modulus of loaded vulcanizates. J Appl Polym Sci 3:127

Raj RG, Kokta BV, Daneault C (1990) A comparative study on the effect of aging on mechanical properties of LLDPE-glass fiber, mica, and wood fiber composites. J Appl Polym Sci 40:645–655

Ramamurthy AV (1986) Wall slip in viscous fluids and influence of materials of construction. J Rheol 30:337–357

Saheb DN, Jog JP (1999) Natural fiber composites: a review. Adv Polym Technol 18:351–363

Venet C, Vergnes B (1997) Experimental characterization of sharkskin in polyethylenes. J Rheol 41:873–892

Vlachopoulos J, Alam M (1972) Critical stress and recoverable shear for polymer melt fracture. Polym Eng Sci 12:184–192

White JL, Czarnecki I, Tanaka H (1980) Experimental studies of the influence of particle and fiber reinforcement on the rheological properties of polymer melts. Rubber Chem Technol 53:823–835

Wu S (1979) Order–disorder transitions in the extrusion of fiber-filled poly(ethylene terephthalate) and blends. Polym Eng Sci 19: 638–650